Aging studies of CMS Improved Resistive Plate Chambers through spectroscopic and microscopic characterization of irradiated HPL

Felipe R. S. Gonçalves[a], **M. Barroso Ferreira Filho**[b], **Carlos W. A.**[a], **on behalf of the CMS Muon Group**

[a]Universidade Federal do Ceará (UFC); [b]Universidade do Estado do Rio de Janeiro (UERJ)
feliperavi@fisica.ufc.br, mapse.b@cern.ch, paschoal.william@fisica.ufc.br

1. Introduction

The Compact Muon Solenoid detector Resistive Plate Chamber (CMS-RPC) system [1] was designed for muon identification and reconstruction. There are 1056 RPC detectors, covering over 3000 m22. The gas mixture is $C_2H_2F_4$ (95.2%), iC_4H_{10} (4.5%), and SF_6 (0.3%) 40-50% relative humidity. With the High-Luminosity LHC (HL-LHC), luminosity will increase five times, potentially affecting detector properties and introducing non-recoverable aging effects. The existing system is under a longevity study at HL-LHC radiation levels [2]. Additionally, an improved RPC (iRPC) is being installed in the high pseudorapidity region on the 3rd and 4th endcap disks. Thus, it is important to study possible aging effects in iRPC chambers at HL-LHC radiation levels. An aging study was performed with an iRPC prototype from January 2021 to April 2022 [3], accumulating 50 mC/cm^2. Performance tests during beam tests were satisfactory, but increased currents were observed during the radiation campaign. Therefore, this work investigates microscopic and chemical modifications in irradiated High Pressure Laminate (HPL) samples and their possible connection to detector degradation. Samples from linseed-oil-coated HPL electrodes exposed to gamma irradiation were analyzed with Raman spectroscopy and photoluminescence techniques.

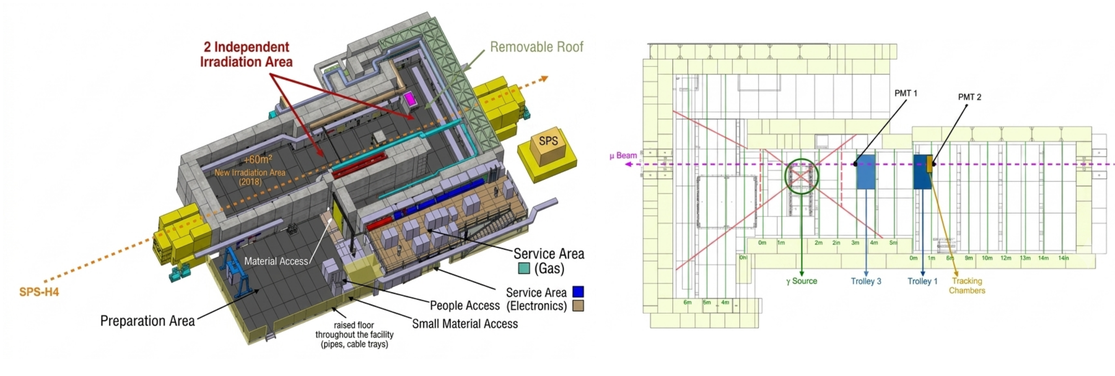

Figure 1: *Left: The GIF++ facility; Right: GIF++ floor plan; the detector under study was installed on trolley 3.*

2. The irradiation campaign

The iRPC detector was set up at the Gamma Irradiation Facility (GIF++). This facility combines a 10.5 TBq 137Cs source with a high-energy muon beam. The prototype is a 1.4 mm double-gap chamber equipped with custom electronics. The irradiation campaign was conducted from January 2021 to April 2022, and the following parameters are well known:

- **Maximum current for each gap:** 130 uA;
- **Currents during the stability:** 50 μA (consistent with the detector operation at the working point);
- **Accumulated charge** → Bottom gap: 52.28 mC/cm^2; Top gap: 50.14 mC/cm^2.

3. iRPC gap details

After the irradiation campaign, the detector was removed from the GIF++ and samples were cut from it. The samples were taken to the laboratory Optical and Electrical Measurements Laboratory (OPEMLab) at the Universidade Federal do Ceará in Brazil, where measurements of the material were performed. A non-irradiated sample was also taken to provide a reference.

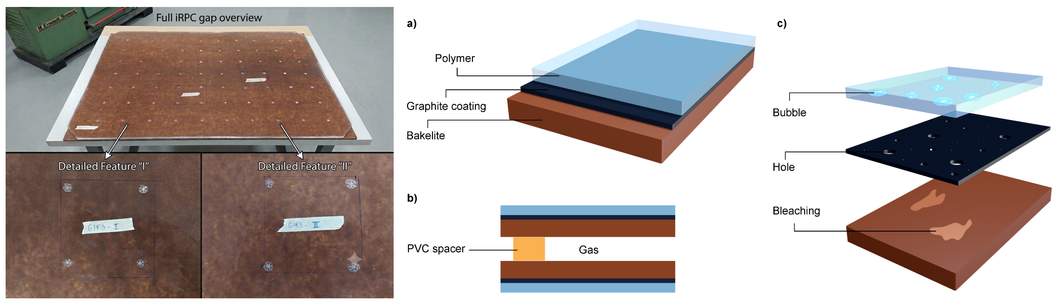

Figure 2: *Left: iRPC gap extracted from the irradiated detector; Right: a) High-pressure laminate (HPL) + graphite coating + polymer; b) RPC gap schematic; c) Defects on an RPC*

4. Spectroscopic and Microscopic characterization

Raman scattering is a non-invasive technique commonly used to characterize materials through their vibrational structure. It consists of illuminating a sample with visible radiation and collecting the frequencies shifted from the incident radiation. The resulting spectrum allows the identification of the vibrational modes of the atom bands in the material. We performed Raman scattering in the plates using a *LabRAM* spectrometer with a 633 nm excitation wavelength.

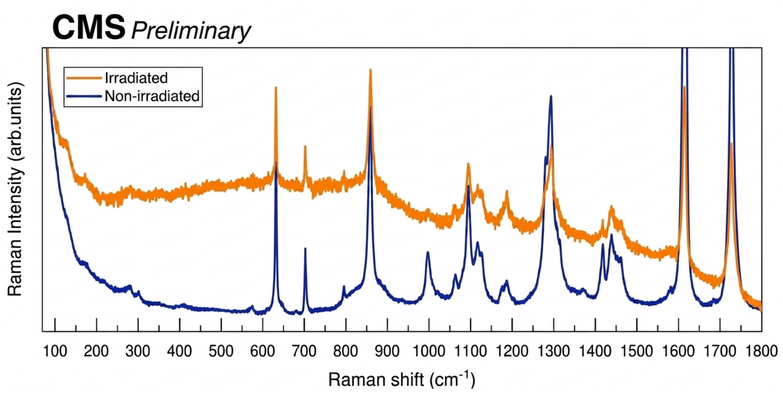

Figure 3: *This plot shows the Raman spectrum for the irradiated and non-irradiated samples. The spectra reveal no significant differences in the vibrational frequencies of the samples. The main difference is the pronounced background in the irradiated sample, attributed to enhanced luminescence under the Raman excitation. This luminescence contribution may reflect changes in the optical emission properties of the material, but the Raman measurements alone do not establish its microscopic origin.*

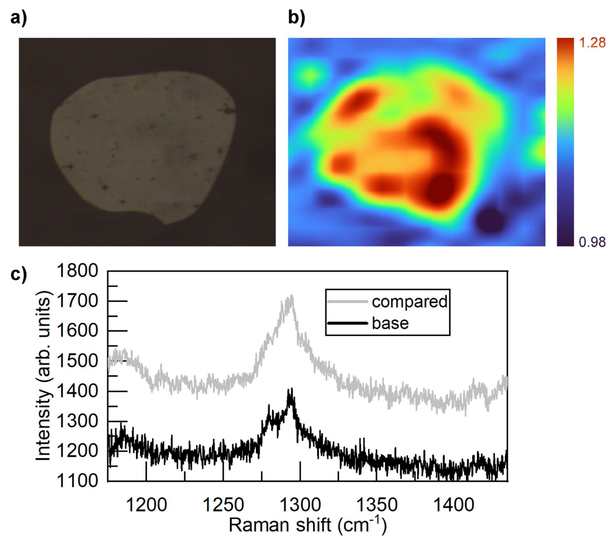

Figure 4: *a)This region shows an optical image of a 400 um bubble in the polyester sheet; b) the respective Raman mappings; c) For completeness, the Raman mapping was performed around the 1300 cm^{-1} peak, since this band may be associated with structural disorder in graphitized materials [5]. In the legend, base is any point in the blue region of the Raman mapping and compared is a point in the red region.*

Photoluminescence can be defined as the emission of light by a material following the absorption of photons. The emission may originate from intrinsic or extrinsic sources, where the first results from interactions between the absorbed photons and the material lattice, and the second, on the other hand, is associated with impurities or defects present in the material [5].

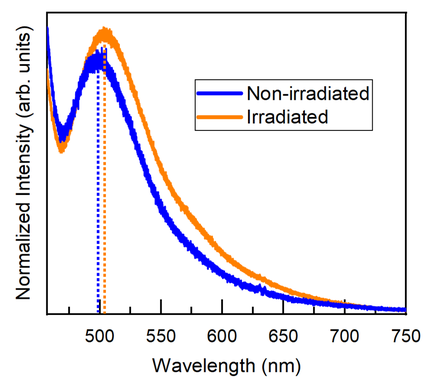

Figure 5: *Compared to the non-irradiated sample, the irradiated RPC spectrum shows a slight redshift, about 5 nm, and enhanced emission intensity around 505 nm. Such spectral modifications are compatible with radiation-induced degradation processes and corroborate observations reported for other polymer systems [4]. It can certainly contribute to the formation of dark currents in the material, reducing the detection sensitivity. As a result, the signal-to-noise ratio may deteriorate, limiting the device's ability to detect weak signals and compromising its overall performance.*

Radiation-induced degradation in RPCs is not fully understood. Bakelite contains residual NaOH and H_2O, while linseed oil contains unsaturated triglycerides. The sodium ions can interact with the oxidized linseed oil through the ionization of carboxylic acid groups:

$$\mathrm{R{-}COOH} \rightarrow \mathrm{R{-}COO^- + H^+}.$$

The resulting carboxylates react with Na^+, while SF_6 hydrolysis provides HF, ultimately yielding:

$$\mathrm{R{-}COONa + HF} \rightarrow \mathrm{R{-}COOH + NaF}.$$

NaF formation may enhance photoluminescence and contribute to bubbles, holes, and bleaching in RPCs.

5. Conclusion

The Raman measurements showed no significant differences in the vibrational frequencies between irradiated and non-irradiated RPC resistive plates. The Raman mapping around the 1300 cm^{-1} band also showed relatively small variations. From the photoluminescence, the irradiated Bakelite showed a 5 nm redshift and increased emission intensity around 505 nm. These changes are consistent with radiation-induced degradation, with no significant impact on iRPC performance. It is worth mentioning that the mechanisms responsible for radiation-induced defects are still not fully understood. Consequently, the next step in this analysis is to compare the performance plots for both iRPC gaps with the Raman and photoluminescence results to identify patterns that could elucidate the aging phenomena.

References

[1] CMS collaboration, The CMS Experiment at the CERN LHC, JINST **3**, S08004 (2008).

[2] CMS collaboration, The Phase-2 Upgrade of the CMS Muon Detectors, Tech. Rep., **CMS-TDR-016**, (2017).

[3] Ferreira Filho, M. Barroso, et al. "Aging studies for the CMS improved Resistive Plate Chambers." Nuclear Instruments and Methods in Physics Research Section A: Accelerators, Spectrometers, Detectors and Associated Equipment 1055 (2023): 168451.

[4] Bedjaoui, S., et al. "XRD, Raman and photoluminescence study of gamma-irradiated PBT." Applied Physics A 128.4 (2022): 365

[5] Pelant, Ivan, and Jan Valenta. Luminescence spectroscopy of semiconductors. Oxford University Press, 2012

Thanks to all colleagues involved in this work and